E3S Web of Conferences **360**, 01075 (2022) https://doi.org/10.1051/e3sconf/202236001075
VESEP2022

Modeling H-bridge inverter based on PI control and its nonlinear dynamic behaviour

Tian Ding, *Yanchi* Zhang*, *Pengfei* Ju, *Wanting* Liao, and *Jun* Fang

School of Electrical Engineering, Shanghai Dianji University, 201306 Shanghai, China

Abstract. In the H-bridge inverter, the control and circuit topology parameters are the key factors affecting its dynamic stability, and the changes of each parameter have different effects on the stability of the system. This paper takes the current-controlled first-order H-bridge passive inverter based on PI control as the research object. Firstly, based on the different modal of the circuit, an accurate discrete iterative mapping model of the H-bridge inverter is derived according to the stroboscopic mapping principle. Then iterate through the above iterative formula, after retaining the data of the current peak value, the dynamic bifurcation diagram on the control parameters of the system is obtained, with the bifurcation behavior and stable working area of the system being analysed when the control parameters change, and verified by the current folding diagram the correctness of the analysis. Finally, according to the same method, the influence of other parameters on the system stability is studied. The research results show that when different parameters change, there are critical maximum or minimum values to keep the system running stably.

1 Introduction

Under the background of the carbon neutrality and carbon peaking goal proposed by China, the traditional power system gradually presents the characteristics of the high proportion of new energy and power electronic devices. The innovation of the power system also brings many new stability problems[1-2]. Therefore, it's necessary to study the dynamic mechanism of power systems containing power electronic devices.

The H-bridge is widely used in modern power electronic systems as an interface for connecting DC and AC sides. Its dynamic stability determines whether the DC/AC system can operate normally or not. A.I. Andriyanov studied of nonlinear dynamics of converters with two types of sinusoidal unipolar reversible modulation[3-4] and a control system based on target-oriented control. Reference [5] mentioned that the oscillatory behavior of single three-phase VSI is studied in the presence of resistive loads. In Reference [6], the switching dynamics of a DC/AC resonant self-oscillating inverter is considered.

This paper takes the first-order H-bridge inverter as the research object. Firstly, the model of the system is established, and the state equation of the system is obtained by analysing the different modes of the circuit, and then the precise discrete iterative formula of the system is obtained by combining the PI control method. With the help of iterative formula, the dynamic

---

* Corresponding author: zhangyc@sdju.edu.cn

bifurcation diagram of the system when the control parameters are changed is obtained, the nonlinear dynamic behavior of the system is analysed, and the folding diagram is used to prove it. Finally, the remaining system parameters are also analysed similarly, and the stability region of each parameter when the system is running normally is obtained, which provides a certain reference for the parameter design of the H-bridge inverter.

2 The topology of first-order H-bridge inverter

Firstly, the topology of the research object is given as shown in Fig. 1. It's mainly composed of the following three parts: (1) DC voltage source; (2) H-bridge inverter; (3) Resistive inductive load.

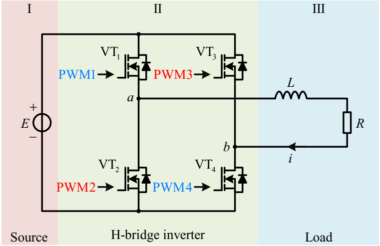

Fig. 1. The topology of first-order H-bridge inverter.

3 System modeling

In order to get the model of the system, after giving the topology of the system, we need to analyse the control method of the system and the different modals it brings. In this paper, the PI control method is used to control the load current $\boldsymbol{i}$ in a closed loop. The two groups of switches are turned on alternately, and their control block diagrams are respectively shown in Fig. 2(a-i) and (a-ii).

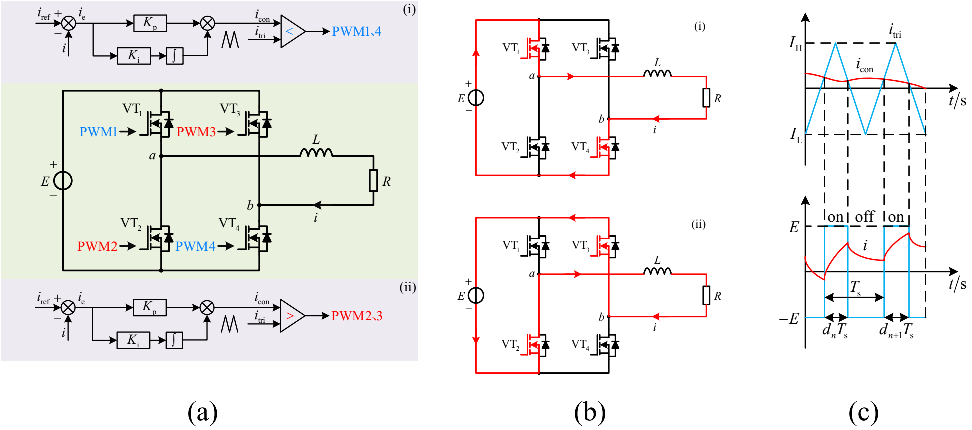

Fig. 2. Control block diagram, two modals' topology and SPWM Schematic; (a) the control block diagram of system with SPWM; (b) the topology of different modals; (c) Schematic diagram of SPWM.

Shown in Fig. 2(a), $\boldsymbol{i}_{\mathbf{tri}}(t)$ and $\boldsymbol{i}_{\mathbf{con}}(t)$ are respectively the triangular carrier signal and the SPWM modulation signal. They are shown in equation (1) during each switching period $\boldsymbol{T}_{\mathbf{s}}$:

$$i_{\mathrm{tri}}(t)=\begin{cases} I_{\mathrm{L}}+4I_{\mathrm{H}}\dfrac{t}{T_{\mathrm{s}}}, & 0<t\le\dfrac{T_{\mathrm{s}}}{2} \\ I_{\mathrm{L}}+4I_{\mathrm{H}}\dfrac{T_{\mathrm{s}}-t}{T_{\mathrm{s}}}, & \dfrac{T_{\mathrm{s}}}{2}<t\le T_{\mathrm{s}} \end{cases} \tag{1}$$

$$i_{\mathrm{con}}(t)=K_{\mathrm{p}}(i_{\mathrm{ref}}-i)+K_{\mathrm{i}}\int_0^{T_{\mathrm{s}}}(i_{\mathrm{ref}}-i)\mathrm{d}t$$

Among them, $\boldsymbol{I}_{\mathrm{H}}$ and $\boldsymbol{I}_{\mathrm{U}}$, respectively, stand for the valley and peak of the triangular carrier wave; $\boldsymbol{K}_{\mathrm{p}}$, $\boldsymbol{K}_{\mathrm{i}}$ are the proportional and integral coefficient of PI controller; and $\boldsymbol{i}_{\mathrm{ref}}$ is the reference current.

Fig. 2 (b) illustrates the current conduction path of the inverter in two different modals. According to the above circuit topology and control block diagram, the state equation and discrete mapping iteration model of the first-order H-bridge inverter can be derived in Section 3.1~3.2.

3.1 State equation

After understanding the working mode of the system, we can establish the state equation of the system for subsequent research. Before establishing the equation of state, we firstly note the voltage which between the midpoints of the two bridge arms about the H-bridge is $\boldsymbol{u}_{ab}$, and then define current as positive when the $\boldsymbol{i}$ flows from *a* to *b*. According to the conduction state of the two groups of switches, they can be divided into two modals as follows.

Modal 1: VT_1 and VT_4 are turned on, with VT_2 and VT_3 turned off at the same time when $\boldsymbol{i}_{\mathrm{con}}(t) < \boldsymbol{i}_{\mathrm{tri}}(t)$. The current conduction path is shown in Fig. 2(b-i), the $\boldsymbol{i}$ increases exponentially and the $\boldsymbol{u}_{ab}$ is equal to $+\boldsymbol{E}$. According to Kirchhoff's law, the state equation can be described in equation (2):

$$\frac{\mathrm{d}i}{\mathrm{d}t}=-\frac{R}{L}i+\frac{E}{L} \tag{2}$$

Modal 2: On the contrary, VT_2 and VT_3 are turned on, with VT_1 and VT_4 turned off at the same time when $\boldsymbol{i}_{\mathrm{con}}(t) > \boldsymbol{i}_{\mathrm{tri}}(t)$. The current conduction path is shown in Fig. 2(b-ii), the $\boldsymbol{i}$ increases exponentially and the $\boldsymbol{u}_{ab}$ is equal to $+\boldsymbol{E}$. Similarly, the state equation in this case is shown in equation (3):

$$\frac{\mathrm{d}i}{\mathrm{d}t}=-\frac{R}{L}i-\frac{E}{L} \tag{3}$$

The equations (2~3) above help us derive the exact discrete iterative formulation of the system in section 3.2.

3.2 Discrete mapping model

Based on the preamble, we used the stroboscopic sampling method [7] to establish the discrete model of the H-bridge inverter in this section. It lays the foundation for the subsequent analysis using the bifurcation diagram. The Schematic diagram of SPWM control with load voltage and current waveforms is shown in Fig. 2(c).

Suppose the working time of modal 1 is $\boldsymbol{t}_n$, and define the duty ratio $\boldsymbol{d}_n=\boldsymbol{t}_n/\boldsymbol{T}_{\mathrm{s}}$, hence the working time of modal 2 is $(\mathbf{1}-\boldsymbol{d}_n)\boldsymbol{T}_{\mathrm{s}}$.

Let the $\boldsymbol{i}$ at the time $\boldsymbol{nT}_{\mathrm{s}}$ is $\boldsymbol{i}_n$, thus the $\boldsymbol{i}$ at the time of $(\boldsymbol{n}+\mathbf{1})\boldsymbol{T}_{\mathrm{s}}$ can be obtained as equation (4) according to equations (2~3) in section 3.1:

$$i_{n+1} = p_1 i_n + p_2 U_\mathrm{d} \tag{4}$$

Among them, $p_1 = e^{-\frac{T_\mathrm{s}}{\tau}}$, $p_2 = \frac{1}{R}[p_1(2e^{\frac{d_n T_\mathrm{s}}{\tau}} - 1) - 1]$, $\tau = \frac{L}{R}$.

Applying different control strategies to the system will give the system different duty ratio expressions. The $\boldsymbol{d_n}$ has the characteristic of saturation[7], its saturation characteristic and expression based on PI control are given according to equation (5):

$$d_n = \begin{cases} 0 & (d_n \le 0) \\ \frac{1}{2}(1 + \frac{i_\mathrm{con}}{I_\mathrm{H}}) & (0 < d_n < 1) \\ 1 & (d_n \ge 1) \end{cases} \tag{5}$$

Among them, the SPWM modulation signal $\boldsymbol{i_\mathrm{con}}$ is as equation (6):

$$i_\mathrm{con}(n) = K_\mathrm{p}(i_\mathrm{ref} - i_n) + K_\mathrm{i} T_s \sum_{k=1}^{n} (i_\mathrm{ref} - i_n) \tag{6}$$

The above equation (4~6) constitutes the exact discrete iterative formula of the system. It can be used in the next section to analyse the influence of different parameters on the normal operation of the inverter.

4 Influence of system parameters on operation

With the preamble, we can analyse the dynamic behavior of a typical inverter nonlinear in this section. The initial design parameters of the system in Fig. 2 are shown in Table 1. The DC voltage $\boldsymbol{E}$ is 220V, and the reference current $\boldsymbol{i_\mathrm{ref}(t)}$ is $\mathbf{5sin(100\pi t)\ A}$. The step size of iterative calculation is 0.5μs, the load current's initial condition $\boldsymbol{i_1}$**=0.5A**, **200** iterations are performed in each switching period, with a total of **50** sinusoidal periods are iterated. According to the principle of Strobe mapping, the sampling period is the switching period of the circuit. The dynamic bifurcation diagram obtained by using the current's peak of the last **20** sinusoidal periods can be applied to the effect of different parameters on the normal operation of the system.

Table 1. System initial design parameters.

Parameter	Definition	Value
E	DC voltage	220V
L	Inductance value of load	15mH
R	Resistance value of load	10Ω
f_s	Switching frequency	10kHz
T_s	Switching period	100μs
$i_\mathrm{ref}(t)$	Reference current	5sin(100πt) A
K_p	Proportional coefficient	1
K_i	Integral coefficient	200
I_H	The peak of the triangular carrier	1

The following section 4.1~4.2 studies the influence of different parameters on the system operation.

4.1 Influence of control parameters on system operation

For the closed-loop control system, the control parameters are very important. Therefore, we first study the nonlinear dynamic behavior of the system when K_p and K_i change. The results are shown in Fig. 3. Fig. 3(a) depicts the dynamic bifurcation diagram of the current peak as K_p varies from 0.4 to 5; the folded diagram[7-8] of the current is shown in Figure 3(b~d), which verifies the nonlinear dynamic behavior of the system. According to the change of the bifurcation parameter K_p, the specific analysis is carried out below.

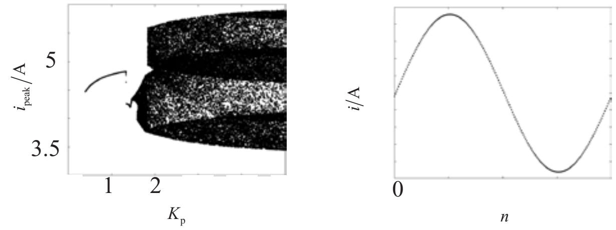

(a) (b) $K_p = 0.5$

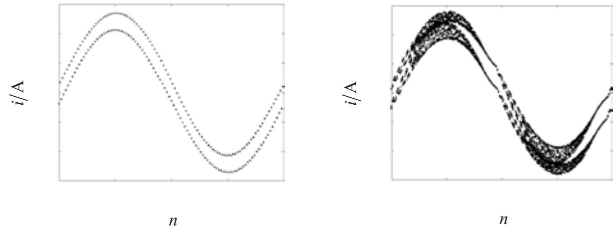

(c) $K_p = 1.4$ (d) $K_p = 2$

Fig. 3. The dynamic bifurcation and folding diagram for K_p; (a) Dynamic bifurcation diagram of peak current with respect to K_p; (b)~(d) the current folding diagram when K_p takes different values.

It can be seen from Fig. 3(a) that in the process of increasing the proportional coefficient K_p from 0.4 to 5, the peak of the load current gradually approaches the amplitude of the given current, and the system gradually changes from a stable state to a period-doubling bifurcation state, and finally enters a chaotic state suddenly, which intuitively describes the nonlinear phenomenon in the inverter. When $0.4< K_p < 1.34$, the sampling points overlap into one point, and it can be seen that the inverter is in a stable operation state; when $1.34< K_p < 1.51$, the sampling results become two curves, and the inverter has a period-doubling bifurcation phenomenon; When $K_p >1.51$, there are many points of indeterminate value at the sampling point, and a self-similar structure appears. It can be seen that the inverter has entered a chaotic state at this time. The analysis of Fig. 3(a) shows that the stability domain of the proportional coefficient K_p is [0.4, 1.34].

Correspondingly, it can be seen from Fig. 3(b) that when $K_p = 0.5$, each sampling point of all sine waves overlaps, and the folding diagram appears as a stable and smooth sine curve, indicating that the inverter is in a stable period 1 state at this time; It can be seen from Fig. 3(c) that when $K_p = 1.4$, the folding diagram appears as two sinusoids, and the system appears period-doubling bifurcation, indicating that the inverter is in the period 2 state at this time; from Fig. 3(d), it can be seen that, when $K_p = 2$, the sampling points are densely distributed in most areas of the folding diagram, indicating that the inverter is in a chaotic state. It can be seen that the conclusion of the folding diagram is consistent with the system stability, bifurcation and chaotic regions divided in Fig. 3(a), which further reflects that the discrete iterative model of the H-bridge inverter which established in section 3.2 is correct.

Similarly, we continue to analyse the influence on the system operation when the integral coefficient is changed. When $0 < K_i < 3635$, the inverter is in a stable operation state; when

$3635 < K_i < 4500$, the inverter appears period-doubling bifurcation; when $K_i > 4500$, the inverter enters a chaotic state. The analysis of Fig. 4(a) shows that the stability domain of the integral coefficient K_i is (0, 3635]. Fig. 4 (b~d) is the corresponding folding diagram.

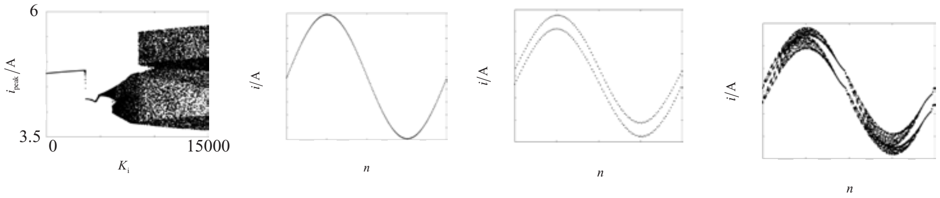

(a) (b) K_i =3500 (c) K_i =4000 (d) K_i =10000

Fig. 4. The dynamic bifurcation and folding diagram for K_i; (a) Dynamic bifurcation diagram of peak current with respect to K_i; (b)~(d) the current folding diagram when K_i takes different values.

4.2 Influence of other parameters on system operation

For the H-bridge inverter, its other parameters such as DC voltage E, load resistance value R, load inductance value L, and switching frequency f_s will also affect the stable operation of the system, so it is necessary to study them. According to the research method in Section 4.1, we also obtained the dynamic bifurcation diagram of other parameters. The results are shown respectively in Fig. 5(a~d).

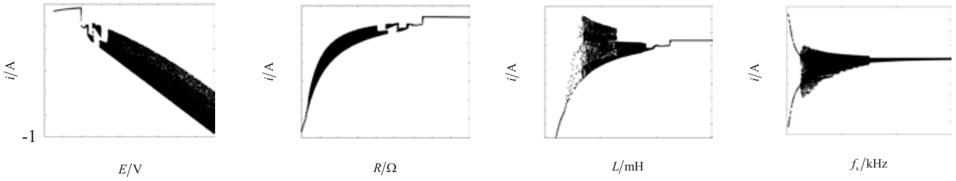

(a) (b) (c) (d)

Fig. 5. The dynamic bifurcation diagram of other parameters.

For the E, as it increases, the system gradually transitions from a stable state to a period-doubling bifurcation state and finally to a chaotic state. On the contrary, the reduction of the remaining three parameters results in a similar nonlinear dynamic behavior of the system.

Based on Fig. 5, we directly give the stable domains of other parameters for H-bridge, as shown in Table 2:

Table 2. The stable domain of other parameters for H-bridge.

Parameter	E	R	L	f_s
Stable domain	[150V, 294V]	[7.5Ω, 10Ω]	[11.5mH, 15mH]	> 7.6kHz

5 Conclusion

In this paper, based on the principle of stroboscopic mapping, the first-order H-bridge inverter is modelled, and its precise discrete iterative formula is deduced according to its different modes and PI control methods. The nonlinear dynamic behavior of the system is analysed by using the dynamic bifurcation and folding diagram, and the stability domain of each parameter of the system is finally revealed. The conclusion is as follows:

(1) For parameters such as proportional coefficient $\boldsymbol{K}_\mathbf{p}$, integral coefficient $\boldsymbol{K}_\mathbf{i}$, and DC voltage $\boldsymbol{E}$, as the parameters increase, the system will gradually transition from single-period steady state to period-doubling bifurcation and finally to chaotic state;

(2) For remaining parameters such as the resistance value $\boldsymbol{R}$, inductance value $\boldsymbol{L}$ and switching frequency $\boldsymbol{f}_\mathbf{s}$, with the decrease of them, similar nonlinear dynamic behavior will also occur in the system;

The stability analysis of different parameters carried out in this paper provides parameter design guidance for the H-bridge inverters, so as to ensure that the DC/AC system can work in the desired single-period stable state. The gradual deepening of the above research and the continuous maturity of research methods make the design of power electronic systems more reliable.

References

1. X. Xie, J. He, H. Mao, H. Li, Proceedings of the CSEE (2021)
2. Q. Jiang, L. Wang, X. Xie, High Voltage Engineering (2017)
3. A. I. Andriyanov, 2017 Dynamics of Systems, Mechanisms and Machines (Dynamics) (2017)
4. A. I. Andriyanov, 2018 International Conference on Industrial Engineering, Applications and Manufacturing (ICIEAM) (2018)
5. E. Ponce, L. Benadero, A. E. Aroudi, L. Martínez-Salamero, 2017 14th International Multi-Conference on Systems, Signals & Devices (SSD) (2017)
6. Y. Li, Z. Li, S. Wong, X. Chen, Z. Chen, X. Liu, 2015 IEEE International Symposium on Circuits and Systems (ISCAS) (2015)
7. X. Wang, B. Zhang, Transactions of China Electrotechnical Society, 103 (2009)
8. X. Wang, B. Zhang, D. Qiu, Acta Physica Sinica, 2251 (2009)